

## COMPUTER SIMULATION OF ELECTROPHORETIC SEPARATION PROCESS

Seungsoo Lee, George S. Dulikravich and Branko Kosovic  
 Postdoctoral Fellow Associate Professor Graduate Assistant  
 Department of Aerospace Engineering, 233 Hammond Building  
 The Pennsylvania State University  
 University Park, PA 16802, USA

### Abstract

A mathematical model for three-dimensional laminar steady flow of an incompressible viscous neutrally charged carrier fluid mixed with an electrically charged fluid was presented. All magnetic fields have been neglected. Thermally induced buoyancy was incorporated via Boussinesque approximation while including Joule heating effect. Numerical results demonstrate detrimental effects of numerical dissipation on the accuracy of the solution. Bending of a stream of charged particles under the influence of an electric field and an electrohydrodynamic instability were successfully demonstrated.

### Mathematical model for EHD flows

Electrohydrodynamics (EHD) and Magnetohydrodynamics (MHD) are representing two extreme models for a general fluid flow under the influence of electromagnetic fields<sup>1-3</sup>. The EHD model assumes that there is no magnetic field applied or induced<sup>4</sup>, while MHD model assumes that there are no charged particles in the flow field and that there is no electric potential applied. In EHD flows external electric field is applied to a fluid containing electrically charged particles. Applications of EHD flows range from ink-jet printers to electrophoretic separation processes<sup>5-9</sup>. Only incomplete models of EHD flows have been numerically solved in the past.

Mathematical model presented in this paper consists of a neutral carrier fluid with a single specie of charged fluid. This model can be easily extended to multi-specie problems including non-neutral carrier fluid. The system of governing equations is derived from a combination of Maxwell's equations of electrodynamics and the Navier-Stokes equations. Idealized charged fluid is assumed and therefore magnetic fields can be neglected. Maxwell's equations reduce to charge conservation equation and equation for electric potential. For computational purposes system of equations can be written in fully conservative vector form in general  $\xi, \eta, \zeta$  curvilinear coordinates as follows:

$$\frac{\partial \tilde{Q}}{\partial t} + \frac{\partial \tilde{E}}{\partial \xi} + \frac{\partial \tilde{F}}{\partial \eta} + \frac{\partial \tilde{G}}{\partial \zeta} = D^2(J\tilde{Q}) + \tilde{H} \quad (1)$$

To make system of equations (1) hyperbolic in time artificial compressibility concept was applied<sup>10</sup> and  $p/\beta$  term was added to mass conservation equation. Solution vector, flux and source term vectors in curvilinear coordinates and non-dimensional form are:

$$\tilde{Q} = \frac{1}{J} \begin{bmatrix} p/\beta \\ u \\ v \\ w \\ \theta \\ q \end{bmatrix} \quad \tilde{E} = \frac{1}{J} \begin{bmatrix} U \\ Uu + \xi_x p \\ Uv + \xi_y p \\ Uw + \xi_z p \\ U\theta \\ q(U + \frac{1}{RePr_e} E_\xi) \end{bmatrix} \quad \tilde{F} = \frac{1}{J} \begin{bmatrix} V \\ Vu + \eta_x p \\ Vv + \eta_y p \\ Vw + \eta_z p \\ V\theta \\ q(V + \frac{1}{RePr_e} E_\eta) \end{bmatrix}$$

$$\tilde{G} = \frac{1}{J} \begin{bmatrix} W \\ Wu + \zeta_x p \\ Wv + \zeta_y p \\ Ww + \zeta_z p \\ W\theta \\ q(W + \frac{1}{RePr_e} E_\zeta) \end{bmatrix} \quad D^2(J\tilde{Q}) = \left[ \frac{S}{J} \tilde{E}_{ij} (J\tilde{Q})_{,j} \right]_{,i}$$

$$\tilde{H} = \frac{1}{J} \begin{bmatrix} 0 \\ \frac{Gr}{Re} n_\xi + Sq E_\xi \\ \frac{Gr}{Re} n_\eta + Sq E_\eta \\ \frac{Gr}{Re} n_\zeta + Sq E_\zeta \\ SEc \left[ q \left( v + \frac{1}{RePr_e} E \right) - \frac{1}{ReDe} \nabla q \right] E \\ 0 \end{bmatrix} \quad (2)$$

$$\nabla^2 \Phi = -Nq \quad (3)$$

where electric field  $E = (E_\xi, E_\eta, E_\zeta)$  is given as  $E = -\nabla \Phi$  (4)

The Jacobian determinant of the geometric transformation from physical into computational space is  $J = \frac{\partial(\xi, \eta, \zeta)}{\partial(x, y, z)}$ ,  $g_{ij}$  is contravariant metric tensor,  $v = (u, v, w)^T$  denotes velocity field with  $U, V$  and  $W$  as its contravariant components,  $p$  pressure,  $q$  charge density,  $\theta$  nondimensional temperature, and  $\Phi$  electric potential.  $S$  is diagonal matrix  $1/Re \text{diag}(0, 1, 1, 1, 1/Pr, 1/De)$ . Non-dimensional numbers Reynolds number  $Re$ , Prandtl number  $Pr$ , Eckert number  $Ec$ , Grashof number  $Gr$  are defined in a standard way while electrical characteristic numbers are:

Charge diffusivity characteristic	Lorentz force characteristic
$De = \frac{\mu}{\rho D}$	$S = \frac{q_r \Phi_r}{\rho v_r^2}$
Electric Prandtl number	Electric field characteristic
$Pr_e = \frac{\mu}{\rho b \Phi_r}$	$N = \frac{q_r L^2}{\epsilon \Phi_r}$

In the equations above  $\rho$  represents density,  $L$  characteristic length,  $\mu$  dynamic viscosity,  $c_p$  specific heat,  $\kappa$  heat diffusivity coefficient,  $\alpha$  thermal expansion coefficient,  $\epsilon$  electrical permittivity, while subscript  $r$  denotes reference values. Diffusivity coefficient  $D$  and mobility coefficient  $b$  are related by the Einstein's relation<sup>4</sup>. It should be noted that the electric permittivity  $\epsilon$  is assumed to be uniform. System of equations given by (1) is solved using four stage Runge-Kutta explicit time stepping method<sup>11</sup>. Second and fourth order artificial dissipation were added to improve the convergence rate.

### Results

The first test case is a simple model for the flow in electrophoresis chamber. Charged fluid is injected at the centerline of the electrically neutral carrier fluid flow. Electric field of 7000 V/m is imposed along the sidewalls. Temperature is constant along the boundaries, Joule's heating and buoyancy force effects are neglected. This example corresponds to electrophoretic separation in microgravity. Reynolds number for the given flow was  $Re=6.67$ , Prandtl number for water was  $Pr=7.9$ . While the electrical characteristics characteristic numbers were  $S=0.15$ ,  $N=0.204$ , and electric Prandtl number  $Pr_e=2.8$ . A non-clustered computational

grid of  $60 \times 30$  grid cells was used. Influence of the imposed electric field on the electric potential field is predominant (Fig. 1). As a consequence of imposed electric field, charged fluid is deflected from the centerline (Fig. 2 and Fig. 3) as it is carried by carrier fluid along the chamber. To improve the convergence rate a small amount of second and/or fourth order artificial dissipation was added. It was shown that even a very small amount of second order artificial dissipation necessary to enhance the convergence rate has a significant effect on the diffusion of the charged particles (Fig. 4 and Fig. 5). The other approach was to force charge density to be non-negative during iterative procedure. This method seems to give much better results, but in that case charges are not conserved and convergence rate is again not satisfactory.

Second test case represents an example of instability induced by the electric field which is analogous to the classical Benard problem. Electroconvective vortices analogous to thermoconvective vortices will be developed if sufficient electrical potential energy can be released by inverting a charged layer. In a closed chamber the charges were initially equally distributed along the lower wall. An external electric field was imposed by means of electrodes along the lower and the upper wall. In this case, Joule's heating and buoyancy force are taken into account. Nondimensional numbers were  $Re=1$ ,  $Pr=1$ ,  $Gr=3000$ ,  $Ec=1$ ,  $S=1$ ,  $N=1000$ ,  $Pr_e=1$ . Temperature was kept constant along the boundaries. The first case shows four equal, well defined vortices induced by the electric field (Fig. 6). When the strength of the imposed electric field is increased vortex pattern shown on Fig. 7 occurs. Charge density contours are shown in Fig. 8. All computations were performed on Cray-YMP computer at NASA Ames Research Center. This work was partially supported by the Center for Cell Research of the Pennsylvania State University.

#### References

- [1] Stuetzler, O. M., "Magnetohydrodynamics and Electro hydrodynamics", *The Physics of Fluids*, Vol. 5, No. 5, pp. 534-544, May 1962.
- [2] Chandrasekhar, S., Hydrodynamic and Hydromagnetic Stability, Dover Publication Inc., New York, 1961.
- [3] Lee, S. and Dulikravich, G. S., "Magnetohydrodynamic Flow Computations in ThreeDimensions", AIAA Paper 91-1, Reno, NV, Jan. 1991.
- [4] Melcher, J. R., Continuum Electromechanics, The MIT Press, Cambridge, 1981.
- [5] Saville, D. A., "The Fluid Mechanic of Continuous Flow Electrophoresis in Perspective", *PhysicoChemical Hydrodynamics*, Vol. 1, pp 297-307., 1980.
- [6] Ivory, C. F., Gobie, W. A., Bekwith, J. B., Hergenrother, R. and Malec, M., "Electromagnetic Stabilization of Weakly Conducting Fluids", *Science*, Vol. 238, pp. 58-61, Oct. 1987.
- [7] Rhodes, H. P., Snyder, R. S., "Preparative Electrophoresis for Space", NASA TP 2777, 1987.
- [8] Bier, M., Palusinski, O. A., Mosher, R. A. and Saville, D. A., "Electrophoresis: Mathematical Modeling and Computer Simulation", *Science*, Vol. 219, Number
- [9] Biscans, B., Hennequin, J. C., Bertrand, J., "Some Aspects of Continuous Flow Electrophoresis in Microgravity", *Acta Astronautica*, Vol. 13, No. 11/12, pp. 705-713, 1986.
- [10] Chorin, A. J., "A Numerical Method for Solving Incompressible Viscous Flow Problems," *Journal of Computational Physics*, Vol. 2, pp. 12-26., 1967.
- [11] Jameson, A., Schmidt, W., and Turkel, E., "Numerical Solutions of the Euler equations by Finite Volume Methods Using Runge-Kutta Time-Stepping Scheme," AIAA paper 81-1259, Palo Alto, CA, June, 1981.



Figure 1. Electric field iso-potential lines in a straight channel

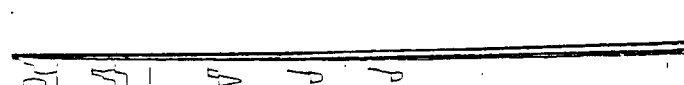


Figure 2. Electric charge density in a straight channel

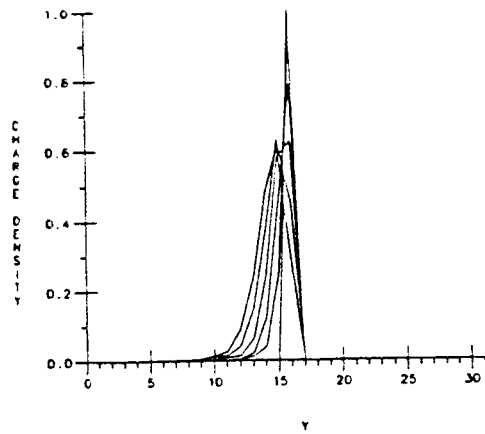


Figure 3. Electric charge density profiles at different stations in a channel



Figure 4. Electric charge density with artificial dissipation

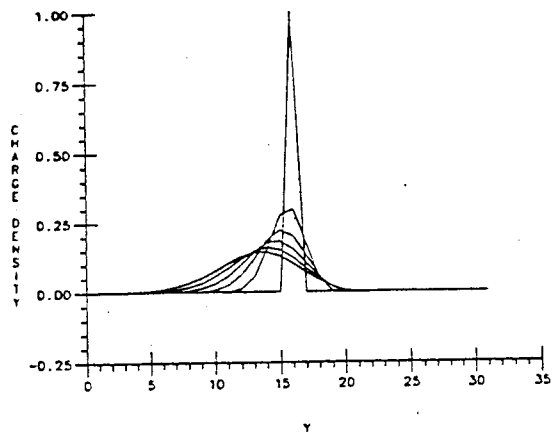


Figure 5. Electric charge density profiles with artificial dissipation

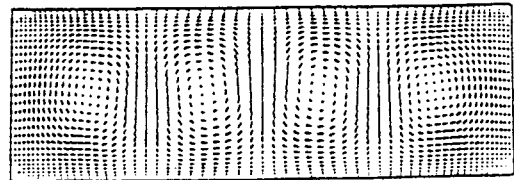


Figure 6. Two pairs of vortices induced by electric field and charged fluid

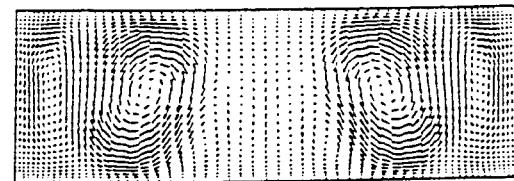


Figure 7. Recirculation having three pairs of electroconvective vortices

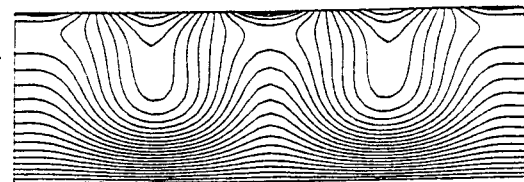


Figure 8. Charge density contours for the three pairs of vortices